FIELD EVALUATION OF A BRIDGE WITH PRECAST UHPC WAFFLE DECK

Ebadollah Honarvar Gheitanbaf, Graduate Research assistant, Department of Civil, Construction, and Environmental Engineering, Iowa State University, Ames, IA
Jon M. Rouse, PhD, Senior Lecturer, Department of Civil, Construction, and Environmental Engineering, Iowa State University, Ames, IA
Sri Sritharan, PhD, Wilson Engineering Professor, Department of Civil, Construction, and Environmental Engineering, Iowa State University, Ames, IA

ABSTRACT

The AASHTO strategic plan in 2005 for bridge engineering identified extending the service life of bridges and accelerating bridge construction as two of the grand challenges in bridge engineering. This study was carried out to investigate the feasibility of utilizing an Ultra High Performance Concrete (UHPC) waffle slab deck, thereby contributing to accomplishing the AASHTO strategic plans.

Following laboratory evaluation of a waffle deck system for bridges and suitable connections, a full-scale, single span, 60 ft long by 33 ft wide demonstration bridge with full depth prefabricated UHPC waffle deck panels was constructed. This paper presents the results from a field testing of the bridge established by subjecting the bridge to static and dynamic truck loads. A 3D ABAQUS finite element model of the bridge was used to help interpret the results of load testing, estimate strains due to dead load, and examine live load distribution. In addition to demonstrating close correlations between measured and expected results, both sets of results confirm structural performance of UHPC waffle slab deck.

Keywords: Ultra-high Performance Concrete (UHPC), Waffle Deck, Live Load Distribution, Accelerated Bridge Construction, Bridge Deck, Field Testing

INTRODUCTION

Each year, more than 3,000 new bridges are constructed in the United States to replace over 150,000 structurally deficient or obsolete bridges[1]. All existing bridges are rated to evaluate their structural performance for new design live loads. Poor bridge deck condition is a leading factor that affects the load rating, implying that deterioration of the deck can make the bridge structurally unsound. Hence, the use of a more durable deck material is likely to significantly increase the service life of bridges.

The use of ultra-high performance concrete (UHPC) as a durable construction material has been receiving more attention as a means to increasing the bridge service life and reducing maintenance costs. The State of Iowa has been a pioneer in implementing the first UHPC bulb-tee and Pi girders in bridges, using UHPC in closure pours for prefabricated superstructure modules[2], and development of an H-shaped UHPC precast pile for foundation applications[3, 4]. Furthermore, full depth UHPC waffle deck panels have been used over the past six years in Europe and the US as an innovative system.

The results and observations from full-scale laboratory tests of UHPC waffle slabs at Iowa State University were used to design a demonstration bridge with a UHPC waffle deck on Dahlonega Road in Wapello County, Iowa[5]. This bridge replacement project was used to demonstrate the deployment of the UHPC waffle slab technology from fabrication through construction. The focus of this paper is to present the evaluation of its performance under true service conditions. The Dahlonega Road Bridge over Little Cedar Creek was opened to traffic in November of 2011 and field tested in February of 2012. The field testing conducted by the Bridge Engineering Center of Iowa State University included monitoring of live load deflections and deformations at discrete, critical locations on the bridge superstructure as it was subjected to static and dynamic truck loads. Figure 1 and Figure 2 show the locations of instrumented panels on the bridge plan and cross section, respectively.

A 3D finite element model of the bridge using ABAQUS software[6] was used to help interpret the results of live load testing, estimate strains due to dead load, and examine live load distribution. During the field test, strains and deflections were measured using surface mounted strain gages and string potentiometers, respectively. The data recorded during the field test captured only the incremental strain and deflection due to live loads, so to estimate the total strain conditions the measured live load strains were superimposed with the dead load strains computed using the finite element model. Throughout this paper, negative values represent compressive strains and downward deflections; positive values represent tensile strains and upward deflections.
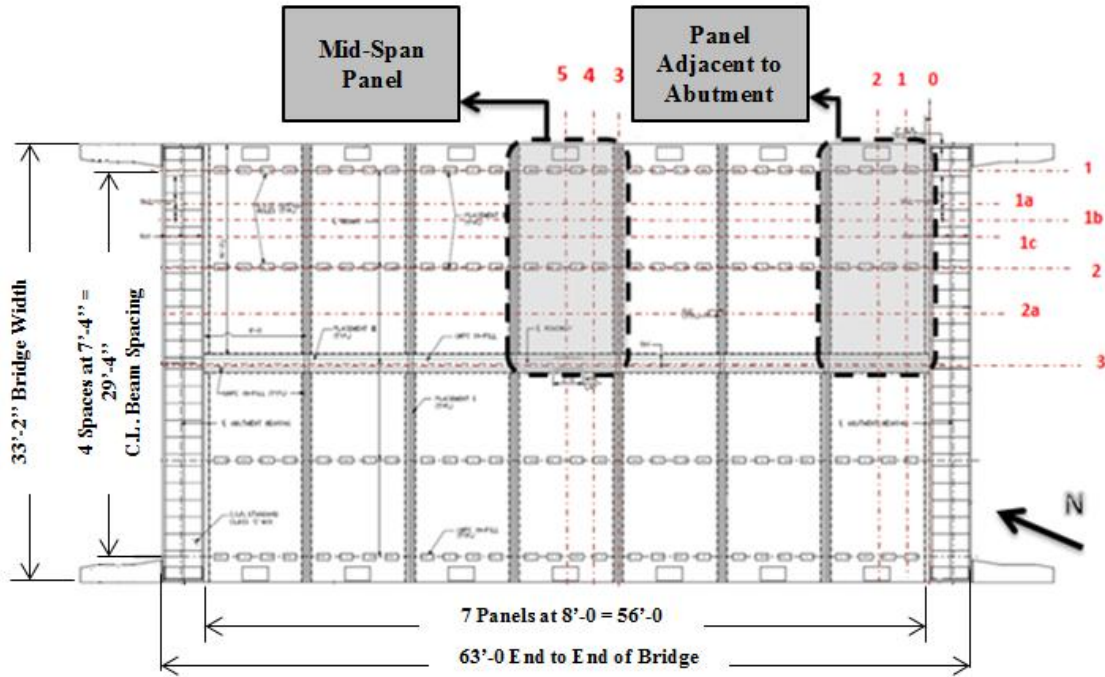
Figure 1: Dahlonega Road Bridge Plan
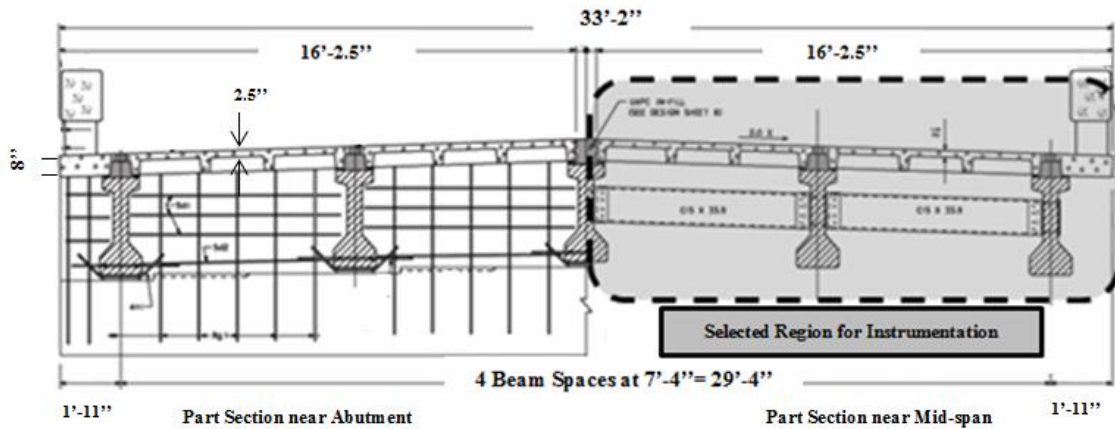
Figure 2: Dahlonega Road Bridge Cross Section

INSTRUMENTATION AND FIELD TEST METHODOLOGY

Taking advantage of the bridge's symmetry about its longitudinal and transverse center lines, two UHPC waffle deck panels along the length of the bridge were selected for instrumentation. One of these panels was located near the mid-span and the other was located adjacent to the south abutment as identified in Figure 1. Both panels were expected to behave similarly, but the panels adjacent to the abutment have slightly different boundary conditions due to end diaphragm. Surface mounted strain gages were used on each panel and their adjacent UHPC deck joints to identify the likelihood of cracking under the applied service loads. The locations of these strain gages were carefully selected to coincide with

critical locations on the panels and deck joints where stress and strain would likely be extreme.

All the strain gages, and string potentiometers were calibrated before performing the field test. The precisions for strain gages, and string potentiometers were 1 micro strain, and a thousandth of an inch respectively.

A total of 15 strain gages were placed on the mid-span panel and surrounding UHPC joints. Eight of these strain gages were located on the bottom of the deck at regions of maximum positive moment, and seven were located on the top of the deck at regions of maximum negative moment. The locations of these gages and their orientations are shown in plan and section views in Figure 3. Of these 15 gages, seven are located either on the UHPC infill deck joint or spanning the interface between the joint and the UHPC precast panel to identify distress in the joint regions or opening of the interface between joint and panel.

Similar to the mid-span panel, a total of 10 gages were placed on the panel adjacent to the abutment and surrounding UHPC joints. Six strain gages were located on the bottom of the deck at regions of maximum positive moment, and 4 were located on the top of the deck in regions of maximum negative moment. The locations of these gages and their orientations are shown in plan and section in Figure 4. Of these 10 gages, 2 are located to span the interface between the UHPC infill joint and UHPC precast panel to identify opening at this interface.

In addition to the strain gages on the deck panels, 13 surface mounted strain gages and 5 string potentiometers were attached to the girders to characterize the global bridge behavior, measure mid-span deflections, and quantify lateral live load distribution factors. Using two additional string potentiometers, deflections were also measured at the mid-spans of the deck panel located near the center of the bridge. Top and bottom girder strains were monitored for 3 of the girders at mid-span and at a section 2 ft. from the southerly abutment.

Each transducer was assigned a name based on its location and orientation. The location is defined by whether it is located near the mid-span or near the abutment, whether it was mounted to the girder or deck, and whether it is located on top or bottom. The orientation is specified relative to the longitudinal or transverse axis of the bridge. The nomenclature for transducers is further explained in Table1. Strain gage and string potentiometer locations are illustrated in Figure 3 and Figure 4 to show exactly where they were placed for the load testing. A photograph of several of the surface mounted strain gages on the bottom of the panel adjacent to the abutment is shown in Figure 5.

Table 1: Transducer Nomenclature

| Convention		
	Span Location	
First Digit	M	Mid-Span
	A	Near Abutment
	Deck/Girder	
Second Digit	G	Girder
	D	Deck
	Direction	
Third Digit	L	Longitudinal
	T	Transverse
	Top/Bottom	
Fourth Digit	T	Top
	B	Bottom
Fifth Digit	**Longitudinal Grid Number ***	
Sixth Digit	**Transverse Grid Number ***	

* See bridge plan in Figure 1 for grid locations

Example: **MDTT13**: **M**id-span **D**eck panel, oriented **T**ransversely on **T**op along longitudinal grid line 1 and transverse grid line 3
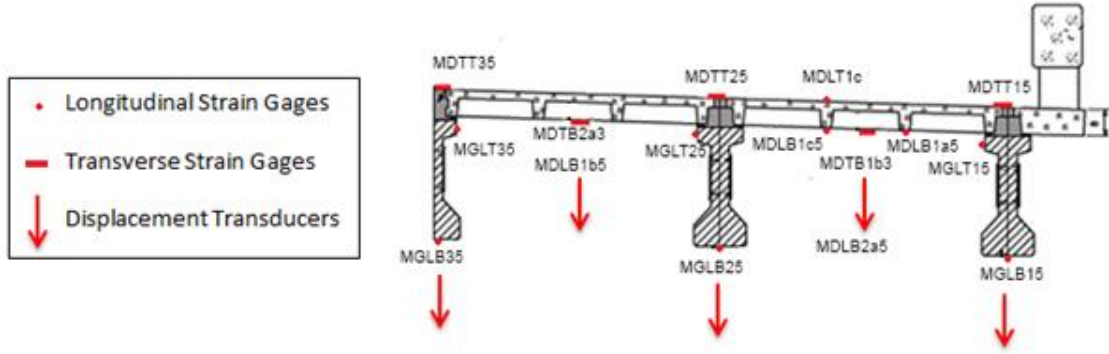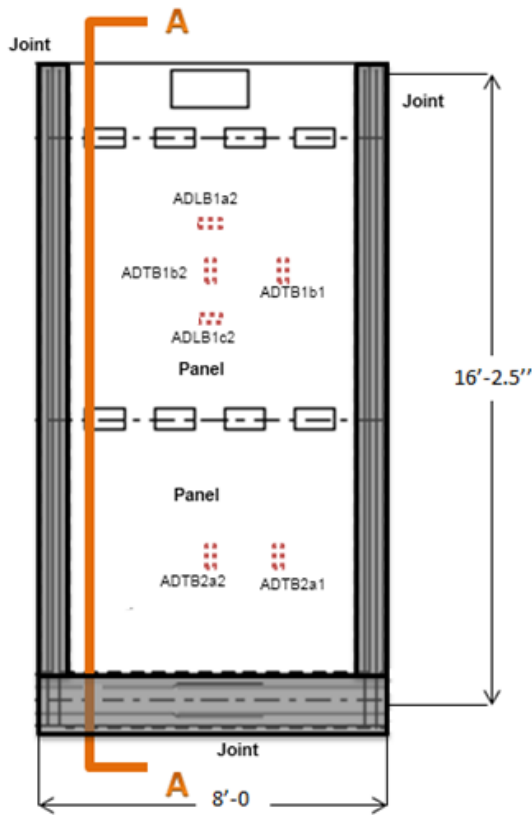
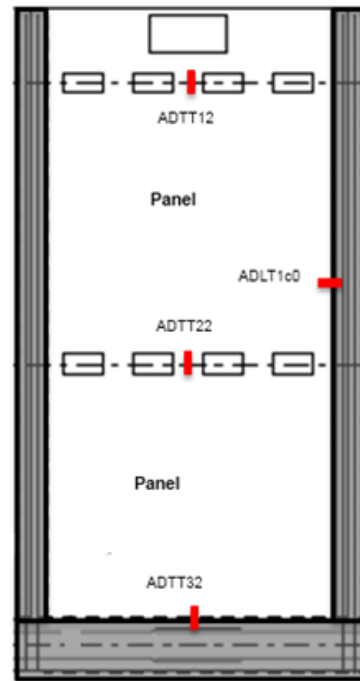## INSTRUMENTATION FOR MID-SPAN PANEL
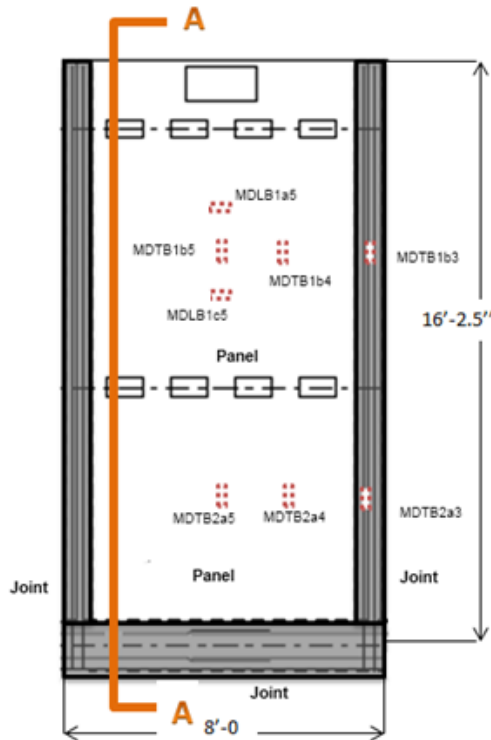
Figure 3(a)
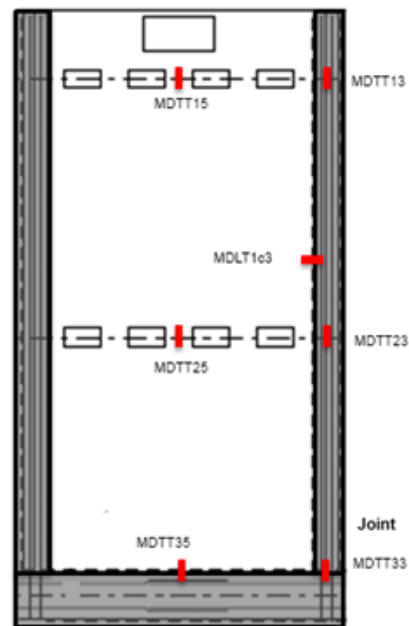
Figure 3(b)

Figure 3(c)
Figure 3: Location of Transducers at Mid-Span Panel: (a) Bottom of Deck, (b) Top of Deck, (c) Cross Section View
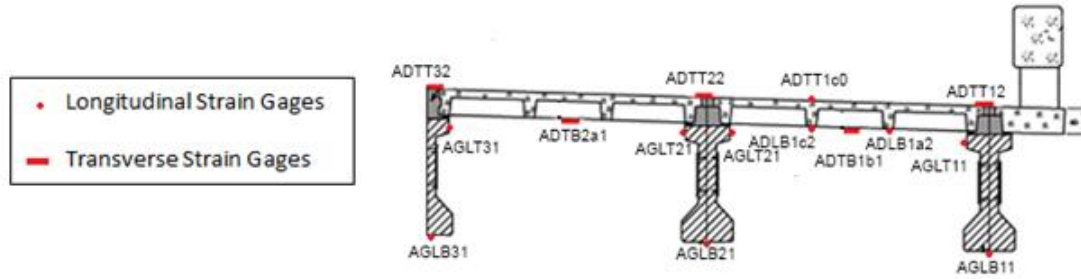
INSTRUMENTATION FOR PANEL ADJACENT TO ABUTMENT

Figure 4(a)   **Figure 4(b)**

Figure 4(c)

Figure 4: Location of Transducers at Panel Adjacent to Abutment: (a) Bottom of Deck, (b) Top of Deck, (c) Cross Section View

Live load was applied to the bridge by driving a heavily loaded dump truck across the bridge along predetermined paths. The total weight of the truck was 60,200 lbs with a front axle weight of 18,150 lbs and two rear axles weighing roughly 21,000 lbs each. The truck configuration with axle loads is shown in Figure 6.

Seven load paths were used for this test as shown in Figure 7. Load paths 1 and 7 were two feet from each barrier rail for the outer edge of the truck. Load paths 2 and 6 were along the centerline of each respective traffic lane. Load paths 4 and 5 were two feet to either side of the bridge centerline for the outer edge of the truck, and load path 3 straddled the centerline of the bridge. To guide the truck driver, lines were painted on the bridge deck along the load paths as shown in Figure 8.

For static load tests, the truck was driven across the bridge at a crawl (speed < 5 mph). Each load path was traversed twice to ensure repeatability of the measured bridge response. For all dynamic tests, the truck speed was increased to 30 mph to examine dynamic amplification effects.

Figure 5: Transducers under Deck Adjacent to Abutment Face
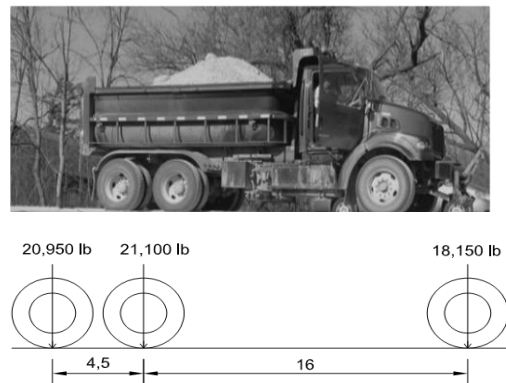
Figure 6: Truck Configuration and Axle Weights
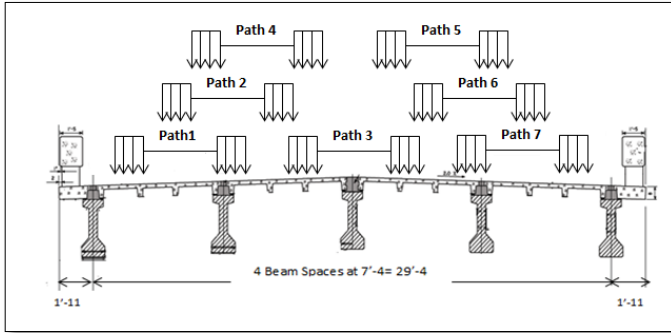
Figure 7: Schematic Layout of
Bridge Loading Paths

Figure 8: Load Paths Marked
on Bridge Deck

FIELD TEST REULTS

The response of the bridge to a slowly moving truck load along the seven prescribed load paths is summarized. Maximum responses for the 14 truck passes executed (two per load path to ensure repeatability) are presented. Because the load test captures only incremental live load deformations, the total strains presented were computed by superimposing the dead load strains computed with the finite element model of the bridge with the measured live load strains from the load test. For the deck panels the dead load strains typically comprise only a minor portion of the total strains because the waffle slab panels are so light relative to a conventional cast-in-place concrete deck.

MAXIMUM STRAINS OF THE MID-SPAN DECK PANEL

The maximum strains observed for each load path at the panel adjacent to the bridge abutment are presented in Tables 5 to 8. Unlike at the mid-span panel, some hairline cracks were observed on the bottom of the ribs on the panel adjacent to the south abutment prior to loading. Consequently, relatively higher strains in the order of 250 µε were observed at these locations (e.g. gages ADTB2a2 and ADLB1a2 – see Tables 5 and 8) during the live load test when compared to strains in the mid-span panel. These strains are comparable to the expected cracking strain of the UHPC and are smaller than the maximum strains observed in the laboratory panel tests[7]. Because they are on the bottom of the deck and are not excessive in magnitude, small cracks at these locations are unlikely to pose a threat to the long-term performance of the panel; this behavior is consistent with the assumption made in during design of the bridge deck. These relatively higher strains are examined and discussed more thoroughly later with the aid of the finite element model.

Table 2: Maximum Transverse Strains at the Bottom of Mid-span Panel

	Load Path Number						
	1	**2**	**3**	**4**	**5**	**6**	**7**
Location	MDTB1b4	MDTB1b4	MDTB2a4	MDTB2a4	MDTB1b4	MDTB1b4	MDTB1b4
Live load Strain (με)	76	77	69	91	-10	-8	-7
Total Strain (με)	78	79	74	96	-8	-6	-5

Table 3: Maximum Transverse Strains at the Top of Mid-span Panel

	Load Path Number						
	1	**2**	**3**	**4**	**5**	**6**	**7**
Location	MDTT15	MDTT15	MDTT15	MDTT15	MDTT13	MDTT13	MDTT15
Live load Strain (με)	27	46	27	42	5	6	6
Total Strain (με)	40	59	40	55	8	8	19

Table 4: Maximum Longitudinal Strains at the Bottom of Mid-span Panel

	Load Path Number						
	1	**2**	**3**	**4**	**5**	**6**	**7**
Location	MDLB1a5	MDLB1c5	MDLB1c5	MDLB1c5	MDLB1c5	MDLB1c5	MDLB1c5
Live load Strain (με)	-47	-36	-5	-30	-6	-3	-4
Total Strain (με)	-52	-49	-18	-43	-19	-16	-17

MAXIMUM STRAINS OF THE DECK PANEL ADJACENT TO ABUTMENT

The maximum strains observed for each load path at the panel adjacent to the bridge abutment are presented in Tables 5-8. Unlike at the mid-span panel, some hairline cracks were observed on the bottom of the ribs on the panel adjacent to the south abutment prior to loading. Consequently, relatively higher strains were observed at these locations (e.g. gages ADTB2a2 and ADLB1a2 – see Tables 5 and 8) during the live load test when compared to strains in the mid-span panel. However, these strains are comparable to the expected cracking strain of the UHPC (~250με) and are smaller than the maximum strains observed in the laboratory panel tests [5]. Because they are on the bottom of the deck and are not excessive in magnitude, small cracks at these locations are unlikely to pose a threat to the long-term performance of the panel. These relatively higher strains are examined and discussed more thoroughly later with the aid of the finite element model.

Table 5: Maximum Transverse Strains at the Bottom of End Panel

	Load Path Number						
	1	**2**	**3**	**4**	**5**	**6**	**7**
Location	ADTB1b2	ADTB2a2	ADTB2a2	ADTB2a2	ADTB2a2	ADTB2a2	ADTB2a2
Live load Strain (με)	93	267	137	253	-10	-8	-3
Total Strain (με)	98	276	145	261	-2	1	6

Table 6: Maximum Transverse Strains at the Top of End Panel

	Load Path Number						
	1	**2**	**3**	**4**	**5**	**6**	**7**
Location	ADTT32	ADTT12	ADTT12	ADTT12	ADTT12	ADTT12	ADTT32
Live load Strain (με)	17	24	24	33	-5	-3	-2
Total Strain (με)	18	25	26	34	-4	-2	-1

Table 7: Maximum Longitudinal Strains at the Bottom of End Panel

	Load Path Number						
	1	**2**	**3**	**4**	**5**	**6**	**7**
Location	ADLB1a2	ADLB1a2	ADLB1c2	ADLB1a2	ADLB1a2	ADLB1a2	ADLB1c2
Live load Strain (με)	245	109	1	68	-2	-2	2
Total Strain (με)	248	113	2	72	1	1	3

Table 8: Maximum Longitudinal Strains at the Top of End Panel

	Load Path Number						
	1	**2**	**3**	**4**	**5**	**6**	**7**
Location	ADLT1c0	ADLT1c0	ADLT1c0	ADLT1c0	ADLT1c0	ADLT1c0	ADLT1c0
Live load Strain (με)	36	-38	7	-39	-6	-6	-5
Total Strain (με)	34	-40	5	-41	-8	-8	-7

MAXIMUM DEFLECTIONS AT MID-SPAN

The string potentiometers located at the mid-span recorded vertical deflections for different load paths for girders as well as the deck. Table 9 shows the maximum deflections registered for each load path.

Table 9: Maximum Live Load Girder and Deck Deflections (in)

Location	MGLB15	MGLB25	MGLB35	MGLB45	MGLB55	MDLB1b5	MDLB2a5
Load Path 1	-0.04	-0.04	-0.01	0.00	0.00	-0.04	-0.03
Load Path 2	-0.03	-0.04	-0.01	0.00	0.00	-0.04	-0.04
Load Path 3	-0.01	-0.02	-0.03	-0.02	0.00	-0.01	-0.04
Load Path 4	-0.03	-0.04	-0.02	0.00	0.00	-0.04	-0.04
Load Path 5	0.00	0.00	-0.02	-0.04	-0.02	0.00	-0.01
Load Path 6	0.00	0.00	-0.01	-0.04	-0.02	0.00	-0.01
Load Path 7	0.00	0.00	-0.01	-0.04	-0.04	0.00	0.00

In summary, the maximum strains and deflections experienced by the Dahlonega Road Bridge during the static field test were well within expected performance parameters. No strains recorded on the top of the deck indicated a likelihood of cracking or opening of joint interfaces that might adversely affect durability. The only locations where strains approached the expected cracking threshold of the UHPC waffle deck were on the underside of the panel adjacent to the abutment. Cracking was observed by visual inspection at these locations prior to commencing the load tests. These cracks were small in width and the strains recorded during the test were less than those recorded on the laboratory test panels at service load levels. Whether these cracks were caused by vehicular loads or developed at some point during fabrication, shipping or erection is not definitive.

ANALYTICAL ASSESSMENT

A 3D nonlinear finite element model (FEM) was developed using ABAQUS software, Version 6.12. The geometry and reinforcement details were accurately employed in the FEM as well as nonlinear material properties. 3D deformable elements were used to construct the finite element model. The waffle deck, girders, and abutments were meshed using an 8 node linear 3D stress elements (i.e., C3D8R in ABAQUS). The mesh sizes of 2 in., 5 in., and 5in. were assigned to waffle deck, girders, and abutments, respectively. The steel reinforcement in the waffle deck and abutments was modeled assuming no slippage between steel and concrete. Two-node linear 3D truss elements (i.e., T3D2 in ABAQUS) were used to mesh the steel reinforcement with a 2 in. mesh size. The mesh size was chosen such that more realistic stresses and strains are predicted in the critical regions. The girders

are considered to be simply supported on the abutment in the model. The meshed assembly of the model and the truck location for load path 2 are demonstrated in Figure 9 and Figure 10, respectively.

The concrete in the prestressed girders and abutments was defined as an elastic material using the estimated concrete Young's modulus. The UHPC in the deck panels was defined as an inelastic material using the predefined Concrete Damaged Plasticity model in ABAQUS. The stress- strain curve for UHPC in compression was generated for a tested 26 ksi compressive strength for the deck panels. The tensile stress-strain behavior of the UHPC was adopted from results of a direct tension tests on dog-bone shaped UHPC coupons. A steel material model was defined to simulate the mild steel reinforcement properties, with an idealized bilinear stress-strain material model used, based on Young's modulus of 29000 ksi, a yield stress of 60 ksi, an ultimate stress of 90 ksi, and an ultimate strain of 0.12. The stress-strain curves for UHPC under compression and tension used in the model are shown below:

Eventually, the analysis was solved using the Static Riks method in ABAQUS. This method is based on the modified Riks method introduced in early 1980's. The algorithm uses an arc length constraint on the Newton-Raphson incremental solution to satisfy equilibrium at highly nonlinear points along the load-deflection curve such as when the peak load of a member has been reached. Hence, the aforementioned method was employed to capture the material nonlinearity without creating any convergence problems.
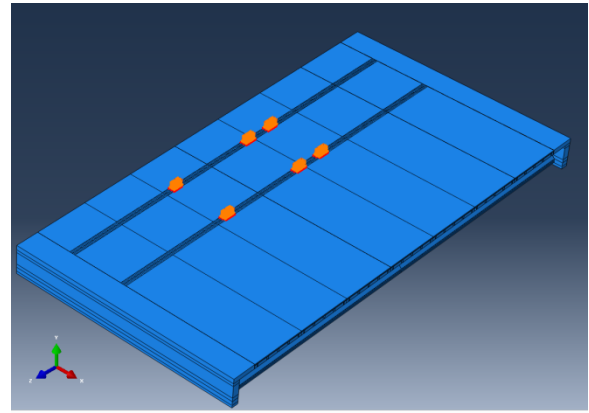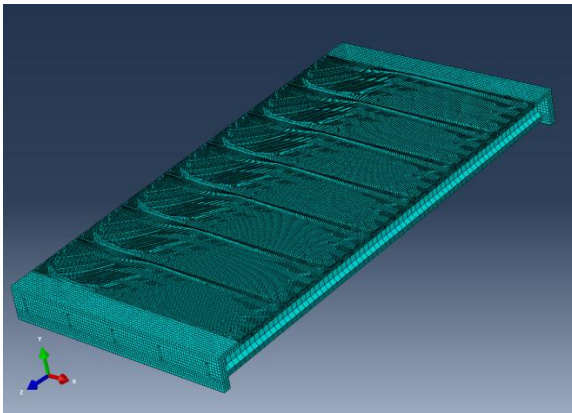
Figure 9: Meshed FEM of the Wapello Bridge   **Figure 10:** Truck Location for Load Path 2
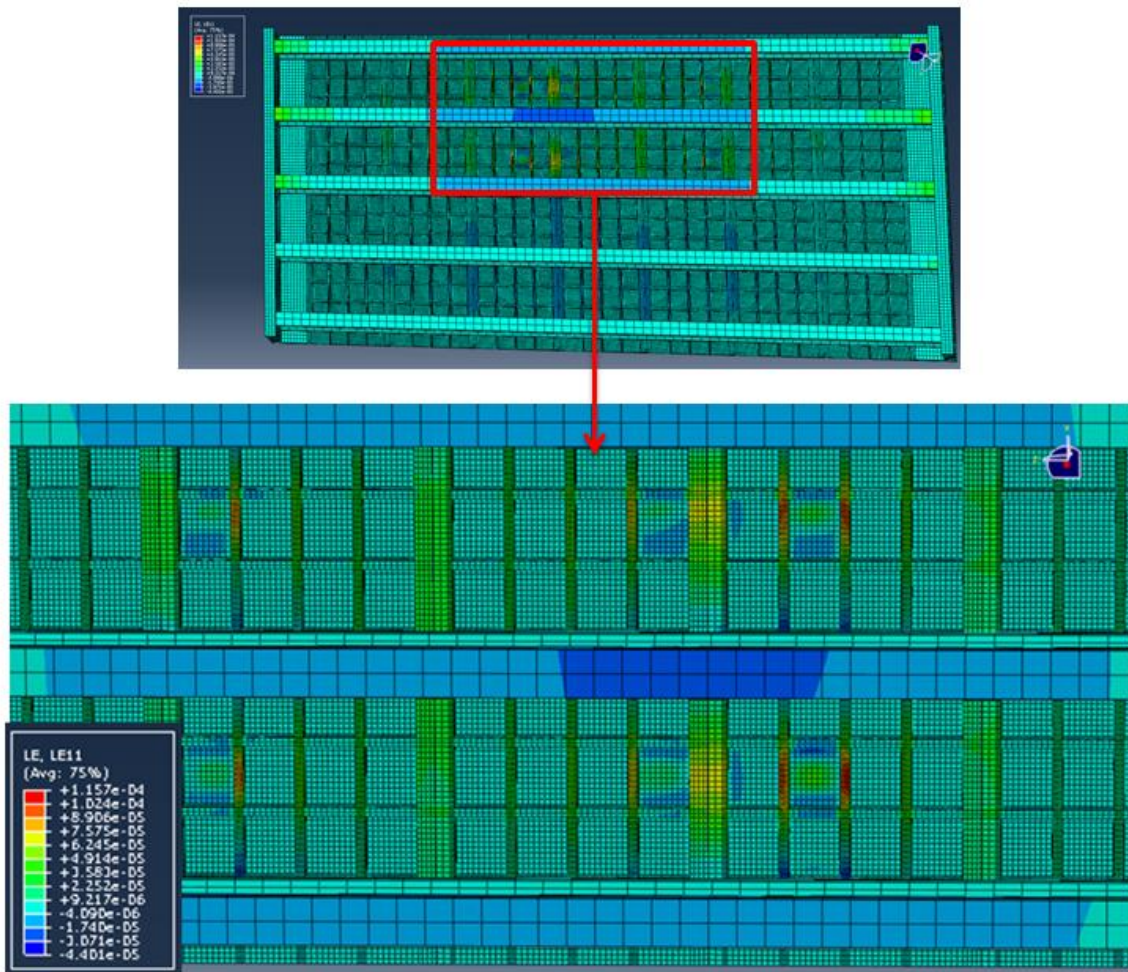
Figure 11: Bottom Transverse Strains for Load Path 2

GLOBAL BRIDGE BEHAVIOR

To assess the finite element model's reliability in predicting the bridge's response to loads applied during the field test, predicted live load deflections and girder strains for load paths 2 and 3 were compared to the corresponding values measured during the test (see Tables 10, 11). The predicted girder deflection and strain values presented in Tables 10, 11 correspond to a critical truck location with the front axle of the truck placed at 52.5 ft from the abutment.

Table 10: Maximum Live Load Girder Deflections

Location	MGLB15	MGLB25	MGLB35	MGLB45	MGLB55
Load Path 2					
Test Results (in)	-0.03	-0.04	-0.01	0.00	0.00
FE Model (in)	-0.04	-0.05	-0.02	-0.01	0.00
Load Path 3					
Test Results (in)	-0.01	-0.02	-0.03	-0.02	0.00
FE Model (in)	-0.01	-0.04	-0.05	-0.04	0.00

Table 11: Girder Top and Bottom Longitudinal Strains at Mid-span

Location	MGLB15	MGLT15	MGLB25	MGLT25	MGLB35	MGLT35
Load Path 2						
Test Results ($\mu\varepsilon$)	17	-3	31	-5	21	-3
FE Model ($\mu\varepsilon$)	21	-3	28	-6	23	-3
Load Path 3						
Test Results ($\mu\varepsilon$)	-8	-3	18	-5	31	-4
FE Model ($\mu\varepsilon$)	-8	-4	22	-7	38	-6

From the Table 10, it is clear that the finite element model predicted maximum live load deflections reasonably well for these two critical load paths for all of the girders. The slight over-prediction of deflection by the model is likely attributable to a small amount of rotational restraint supplied by the concrete diaphragms cast at the ends of the girders over the abutments. In most cases, the model captures actual live load deflection to within 0.01 in.

COMPARISON OF LIVE LOAD STRAINS OF MID-SPAN DECK PANEL

For the live load strains of the mid-span panel (see Tables 12-14), the finite element model was also reasonably effective. The greatest discrepancies of up to 54 $\mu\varepsilon$ for gages MDTB2a5 and MDTB1b5 (see Table 13) could be attributed to slight variations of load placement as the truck was driven across the bridge.

Table 12: Live Load Deck Longitudinal Bottom Strains

Location	MDLB1c5	MDLB1a5
Load Path 2		
Test Results ($\mu\varepsilon$)	-30	-27
FE Model ($\mu\varepsilon$)	-31	-28
Load Path 3		
Test Results ($\mu\varepsilon$)	-3	-3
FE Model ($\mu\varepsilon$)	-4	-4

Table 13: Live Load Deck Transverse Bottom Strains

Location	MDTB2a3	MDTB2a5	MDTB2a4	MDTB1b3	MDTB1b4	MDTB1b5
Load Path 2						
Test Results (µε)	64	21	74	61	77	35
FE Model (µε)	58	75	67	54	72	85
Load Path 3						
Test Results (µε)	14	23	30	-1	-6	-6
FE Model (µε)	12	18	22	0	-3	-5

Table 14: Live Load Deck Transverse Top Strains

Location	MDTT15	MDTT35	MDTT25	MDTT13	MDTT23	MDTT33
Load Path 2						
Test Results (µε)	12	-2	-10	15	7	13
FE Model (µε)	16	-1	-4	12	5	11
Load Path 3						
Test Results (µε)	-4	1	3	-8	1	3
FE Model (µε)	-6	3	5	-11	3	5

COMPARISON OF LIVE LOAD STRAINS OF DECK PANEL ADJACENT TO ABUTMENT

Only at the deck panels adjacent to the abutment did the finite element model predictions vary significantly from the measured live load strains (see Tables 15 and 16). This fact provides evidence that the cracking and elevated strains in this region were most likely caused at some point during fabrication, storage, shipping, or erection. Some preexisting cracks in this location could reduce the moment of inertia of the panel and account for the unexpectedly high strains recorded during the test. If the cracking were due to a large vehicular load, similar damage and strain response would be expected for the mid-span panel as well. If the connection and proximity of the end panel to the abutment were contributing to the elevated strains in this region, the strain recorded by gage ADTB2a1 would also be expected to register a similar strain level which was not the case.

Table 15: Live Load Deck Longitudinal Bottom Strains

Location	ADLB1c2	ADLB1a2
Load Path 2		
Test Results(µε)	64	109
FE Model (µε)	5	9
Load Path 3		
Test Results (µε)	-1	-2
FE Model (µε)	-2	-4

Table 16: Live Load Deck Transverse Bottom Strains

Location	ADTB2a1	ADTB2a2	ADTB1b2	ADTB1b1
Load Path 2				
Test Results (με)	74	267	166	50
FE Model (με)	16	45	27	8
Load Path 3				
Test Results (με)	137	120	-7	-3
FE Model (με)	26	19	-5	-4

Table 17: Live Load Deck Transverse Top Strains

Location	ADTT12	ADTT22	ADTT32
Load Path 2			
Test Results (με)	24	18	5
FE Model (με)	18	15	4
Load Path 3			
Test Results (με)	24	1	-1
FE Model (με)	17	3	-2

GIRDER LIVE LOAD DISTRIBUTION FACTOR

A distribution factor (DF) is the fraction of the total load a girder must be designed to sustain when all lanes are loaded to create the maximum effects on the girder. The distribution factor can be calculated from the load fractions based on either strains or displacement. Load fraction is defined as the fraction of the total load supported by each individual girder for a given load path. Thus, the load fractions for paths 2 and 6 (i.e. when the truck is located at centerline of each respective lane) are calculated based on displacement as below.

$$LF_i = \frac{d_i}{\sum_{i=1}^{n} d_i} \tag{1}$$

where LF_i = load fraction of the ith girder, d_i= deflection of the ith girder, Σd_i= sum of all girder deflections, and n = number of girders.

Hence, the distribution factor for each girder can be computed as below:

$$DF_i = LF_{2i} + LF_{6i} \tag{2}$$

where DF_i =distribution factor of the ith girder, LF_{2i} = load fraction from path 2 of the ith girder, LF_{6i} = load fraction from path 6 of the ith girder.

Table 18: Live Load Distribution Factors for Bridge Girders

Location	MGLB15	MGLB25	MGLB35	MGLB45	MGLB55
LF for Load Path 2	0.38	0.45	0.16	0.01	0.01
LF for Load Path 6	0.01	0.03	0.17	0.50	0.29
DF	0.38	0.49	0.33	0.51	0.30

Also, distribution factors (DF) for interior and exterior girders are computed according to 2007 AASHTO LRFD Bridge Design Specification[8]. Case (k) from AASHTO LRFD Table 4.6.2.2.1-1, precast concrete I section with precast concrete deck might be the most similar to the Dahlonega Road Bridge system. Table 19 shows the results from AASHTO distribution factor equations as well as average distribution factors from Table 18 for interior and exterior girders.

Table 19: Live Load Distribution Factors

Beam	DF AASHTO	DF Displacement
Interior Beams	0.63	0.44
Exterior Beams	0.52	0.34

It is observed that, AASHTO equations overpredict distribution factors for both interior and exterior girders. In other words, the UHPC waffle deck is stiffer than what AASHTO predicts for full-depth precast deck panels.

DYNAMIC AMPLIFICATION EFFECTS

The dynamic test was performed for load paths 2, 3, and 6. The truck was driven at a speed of approximately 30 mph along the bridge to quantify dynamic amplification. The dynamic load allowance, also known as the dynamic amplification (DA), accounts for hammering effects due to irregularities in the bridge deck and resonant excitation as a result of similar frequencies of vibration between bridge and roadway (Interim AASHTO 2008). The 2008 Interim AASHTO LRFD DAF design value is 1.33. Dynamic amplification (DA) can be computed experimentally as follows:

$$DA = \frac{\varepsilon_{dyn} - \varepsilon_{stat}}{\varepsilon_{stat}}$$
(3)

where ε_{dyn} = the maximum strain caused by the vehicle traveling at normal speed at a given location and ε_{stat} = the maximum strain caused by the vehicle traveling at crawl speeds at the corresponding location. The amplification factor (DAF) is then given by:

DAF=1+DA
(4)

Figures 11-13 show the dynamic live load strains experienced by the girders at mid-span for 3 load paths.
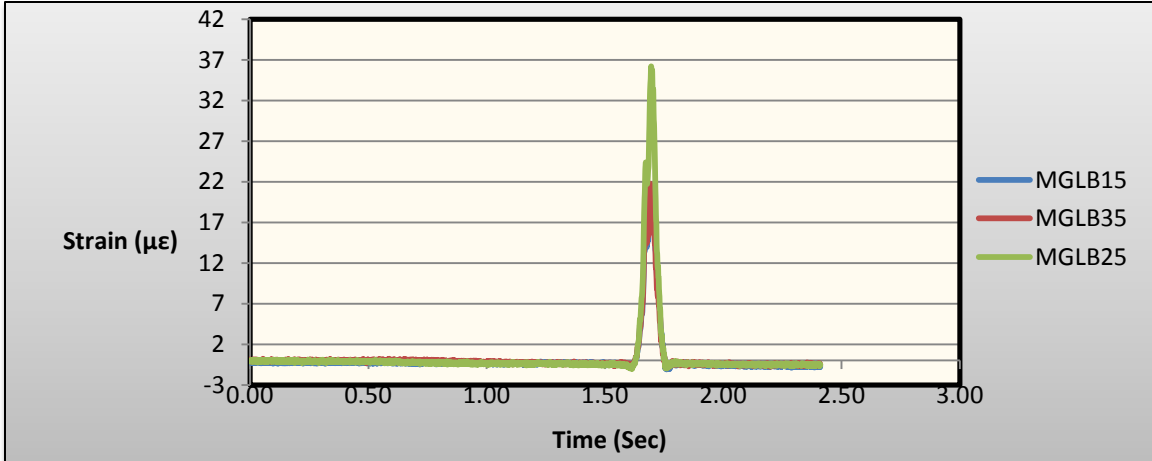
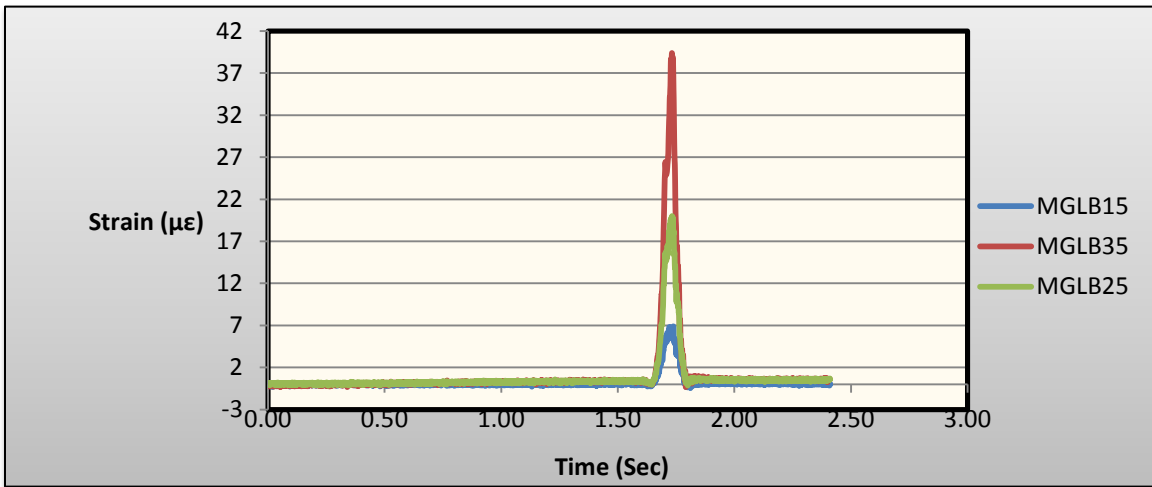**Figure 12:** Dynamic Live Load Longitudinal Strain at Mid-span for Load Path 2

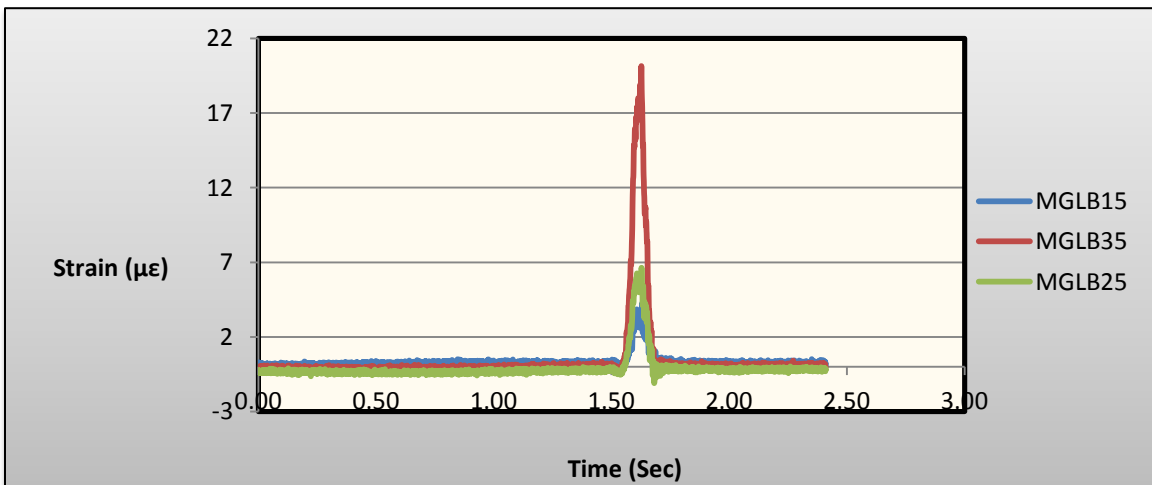**Figure 13:** Dynamic Live Load Longitudinal Strain at Mid-span for Load Path 3

Figure 14: Dynamic Live Load Longitudinal Strain at Mid-span for Load Path 6

Tables 20 and 21 summarize the results for static and dynamic live load strains at the bottom of the girders for three load paths at mid-span. Consequently, the dynamic amplification factor (DAF) may be computed as shown in Table 22. The maximum dynamic amplification computed for the bridge girders is 1.41, slightly greater than the 1.33 recommended by AASHTO for design. This result could be attributable to the relatively light waffle deck as opposed to a solid concrete deck. Also, investigation of dynamic amplification effect for gages on the top of the deck revealed that some gages recorded relatively high DAF's, but none of the dynamic strains approach the assumed cracking strain for UHPC. Gages on the bottom of the waffle deck panels also revealed some mild dynamic amplification effects, but in all cases the dynamic strains were well below those recorded in laboratory tests and deemed acceptable.

Table 20: Summary of Static Live Load Strain (με) for bottom of Girders at Mid-span

Load Path	Transducer		
	MGLB15	MGLB25	MGLB35
Load Path 2	17	31	21
Load Path 3	7	19.	34
Load Path 6	3	7	21

Table 21: Summary of Dynamic Live Load Strain (με) for bottom of Girders at Mid-span

Load Path	Transducer		
	MGLB15	MGLB25	MGLB35
Load Path 2	21	36	22
Load Path 3	7	20	39
Load Path 6	4	7	20

Table 22: Dynamic Amplification Factors

Load Path	Transducer		
	MGLB15	MGLB25	MGLB35
Load Path 2	1.18	1.16	1.04
Load Path 3	1.00	1.04	1.17
Load Path 6	1.41	0.91	0.95

CONCLUSIONS:

According to the field testing of the prototype Dahlonega Road Bridge under static and dynamic truck loads, the following conclusions are drawn about the local and global behavior of the bridge:

- None of the gages placed on the top of the deck registered strains that could indicate any cracking due to the application of live load.

- Preexisting cracks on the bottom ribs of the UHPC waffle slab panel adjacent to the abutment were observed prior to testing. Based on the proper prediction of finite element analysis for other strain gages, it can be inferred that these cracks were likely caused during fabrication, storage, shipping, or erection rather than by vehicular loads, since analytical strains are far below cracking.

- Only two strain gages on the deck panels adjacent to the abutment registered strains greater than the expected cracking strain of the UHPC. Because these strains were not excessive (i.e., less than those measured at service load levels during laboratory testing) and were located on the underside of the deck, no negative impacts to performance are expected.

- None of the strain gages spanning the interface between prefabricated deck panels and their adjacent UHPC infill joints indicated opening of the interface.

- The reduced dead load of the UHPC waffle deck can be beneficial for longer span bridges by decreasing deflection.

- Maximum live load distribution factors for the girders were computed to be 0.5.

- The maximum dynamic amplification factor for the bridge girders was computed to be roughly 1.4.

REFERNCES:

1. Office of Engineering. Federal Highway Administration. U.S. department of Transportation. http://www.fhwa.dot.gov/bridge/deficient.cfm. Accessed 10th February, 2013.

2. Keierleber, B., Bierwagen, D., Wipf, T., and Abu-Hawash, A., "Design of Buchanan County, Iowa Bridge Using Ultra-High Performance Concrete and Pi- Girder Cross Section," Proc. Precast/Prestressed Concrete Institute National Bridge Conference, Orlando, Florida, 2008.

3. Vande Voort, T., Sritharan, S., and Suleiman, "A Precast UHPC pile for Sub structural Applications," In Proceedings of the PCI National Bridge Conference, Phoenix, Arizona, 2007.

4. Vande Voort, T., Suleiman, M. T., and Sritharan, "Design and performance verification of ultra-high performance concrete piles for deep foundations," IHRB Project TR-558 Report, Iowa Department of Transportation, 2008.

5. Aaleti, S., Sritharan, S., Bierwagen, D., and Moore, B, "Precast UHPC Waffle Deck Panels and Connections for Accelerated Bridge Construction," Proc. Of

Precast/Prestressed Concrete Institute National Bridge Conference, Salt Lake City, Utah, 2011.

6. ABAQUS User's Manual, Version 6.11. Dassault Systèmes Simulia Corp., Velizy-Villacoublay, France, 2008.

7. Aaleti, S., Sritharan, S., Bierwagen, D., and Wipf, T., J.,"Experimental Evaluation of structural Behavior of Precast UHPC Waffle Bridge Deck Panels and Connections," Transportation Research Record, Journal of the Transportation Research Board, No. 2251, Transportation Research Board of the National Academies, Washington, D.C., 2011, pp. 82–92.

8. AASHTO LRFD Bridge Design Specifications, American Association of State Highway and Transportation Officials, Washington, D.C., 2007.